

JUNE 29, 2017

USER MANUAL

Afghanistan Transportation Geohazard Risk Management Decision Support System

[HTTP://SPATIAL.MTRI.ORG/WBSS](http://spatial.mtri.org/wbss)



Michigan Tech



User Manual for the Afghanistan Transportation Geohazard Risk Management Decision Support System

June 29, 2017

[HTTP://SPATIAL.MTRI.ORG/WBDSS](http://spatial.mtri.org/wbdss)

Table of Contents

1. Executive Summary.....	6
1.a. DSS Overview.....	7
2. User's Manual.....	11
2. a. Landslide Analysis.....	11
2. b. Avalanche Analysis.....	12
3. Web DSS Interface.....	13
3. a. Overview Window User Interface.....	13
3. a. i. Displaying Hazard and Mitigation Analyses.....	14
3. a. ii. Critical Location Assessment.....	14
3. a. iii. Map Options.....	15
3. b. Analysis Window User Interface.....	15
3. b. i. Accessing the Analysis Window.....	16
3. b. ii. Using the Analysis Window.....	16
3. b. iii. Interpreting the Analysis Window Plots.....	17
3. c. WMS and GIS Integration.....	18
4. Tutorials.....	19
4. a. Interpretation of the factor of safety.....	19
4. b. Determine an optimal mitigation strategy.....	19
4. c. Integrating model results with GeoNode.....	23
5. Troubleshooting.....	25
6. Appendix. Landslide hazard modeling: theory and implementation.....	26
6.a. Models and theoretical background.....	26
6.b. Model inputs and data.....	28
7. References.....	30

Table of Figures

Figure 1. DSS region of interest in Afghanistan	6	Figure 15. Hazard layer with a mitigation area identified using a drawn polygon overlay.	17
Figure 2. DSS showing corridor level earthquake-induced landslide risk	7	Figure 16. Mitigation layer with a mitigation area identified using a drawn polygon overlay.	17
Figure 3. Comparisons of hazard maps with the application of three mitigation strategies.	8	Figure 17. Pixel statistics for unmitigated hazard and mitigated hazard.	18
Figure 4. Hazard zone calculated for the Profile-3 critical location.....	9	Figure 18. A custom critical location added to the overview window.	19
Figure 5. Hazard zone summary calculations	9	Figure 19. A hazard region generated by the DSS at a custom critical location.	20
Figure 6. Avalanche hazard assessment	10	Figure 20. An unmitigated hazard layer shown with a custom critical location and hazard region generated by the DSS in the overview window.	20
Figure 7. The corridor-wide Hazard Analysis dashboard menu	11	Figure 21. Pixel statistics for the hazard region identified at a custom critical location.	21
Figure 8. The 100-year return earthquake-induced shallow landslide hazard West of Doshi	11	Figure 22. Figures generated by the analysis window.....	22
Figure 9. Comparison of a region without (left) and with mitigation (right).....	12	Figure 23. Geonotelanding page	23
Figure 10. McClung and Schaerer's 1981 classification system for avalanche size.	12	Figure 24. Geonote Map for Schools	24
Figure 11. Anatomy of the DSS overview window.	13	Figure 25. Illustration of source and propagation (runout) of landslides.	26
Figure 12. Hazard zone created on the fly for a user-defined point along the corridor.	14	Figure 26. Illustration of the infinite slope model for landslides.	27
Figure 13. Statistics calculated for a hazard zone for 10-year earthquake-induced landslides.	15	Figure 27. Illustration of the three-dimensional rotational model for landslides.	27
Figure 14. Left: anatomy of the DSS analysis window. Right: a fully populated analysis window.	16		

CONTACT

This Decision Support System was developed by Michigan Technological University and the Michigan Tech Research Institute under World Bank Project P160578. The project was led by principal investigator Dr. Robert Shuchman and Dr. Thomas Oommen. The science team members are Dr. Rudiger Escobar Wolf, Michael Battaglia, and Samuel Aden.

1. Executive Summary

The Afghanistan Transportation Geohazard Risk Management Decision Support System (DSS) was created for stakeholders to identify geohazards along transportation corridors in northeastern Afghanistan, and to evaluate the effectiveness of investments in geohazard

mitigation. The DSS was developed specifically for the Baghlan to Bamiyan (B2B) Road and the Salang Highway, two stretches of road that are particularly susceptible to landslides and other geohazards (see Figure 1).

FIGURE 1. DSS REGION OF INTEREST IN AFGHANISTAN



The DSS allows users to visualize geohazards and extreme weather risk, including landslides and avalanches, under a variety of potential scenarios. It also enables users to simulate mitigation techniques to quantify how hazard severity could be reduced if such mitigation techniques are utilized. The DSS incorporates tools to compare and relate the effectiveness of various mitigation procedures for each location along the road. Relative cost estimates for mitigation scenarios are also provided. These functionalities enable the DSS to be integrated

into the normal transport process decision cycles in Afghanistan, from feasibility study to detailed design, as well as operations and maintenance. The DSS can be accessed from the following web link:
<http://spatial.mtri.org/wbdss>

1.A. DSS OVERVIEW

The Salang highway, which connects Kabul to the northern regions of Afghanistan, provides one of the two major land transportation routes through the Hindukush region. The highway reaches elevations of 3400 m and is susceptible to interference and damages resulting from geological and water related hazards. Landslides and avalanches have killed hundreds on the highway over the last several decades. The alternative route for overland travel through the Hindukush is the Baghlan to Bamiyan (B2B) road, which is located at lower altitudes and is generally less susceptible to emergencies related to slope instability and extreme weather. However, B2B is unpaved and almost twice the length of the Salang pass. Travel delays and limitations along these roadways have severe economic implications for Northeastern Afghanistan and Kabul's residents in particular. The DSS was created for the purpose of aiding transportation officials' efforts to plan and mitigate the effects of costly geohazards in the

context of normal transport process. Presented in this report is an executive summary and overview of the DSS, followed by a detailed User's Manual.

The DSS is scalable from the transportation corridor level down to local levels at any point on the road network. Transportation officials can easily visualize corridor-wide geohazard assessments to evaluate large-scale mitigation and investment plan. For example, Figure 2 is a screenshot from the DSS that shows an earthquake-induced hazard for a 100 year return period. On the figure 2, green represents low hazard, yellow represents moderate hazard, and red represents high hazard. This particular analysis allows users to immediately assess where there is a need for large scale mitigation efforts. In the figure below, roughly 100 kilometers of the ~250 kilometer corridor is classified as "low" hazard for an earthquake magnitude that has a 100-year return period thus requires little or no mitigation.

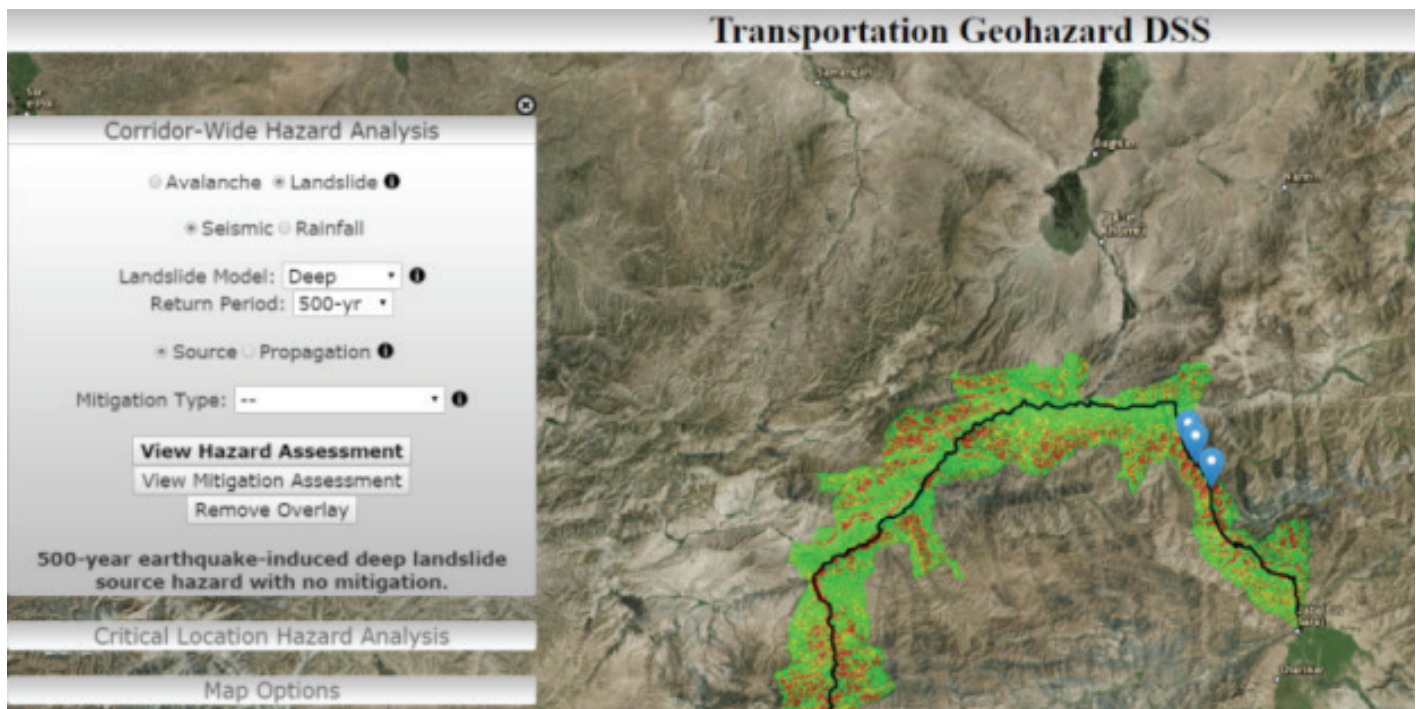


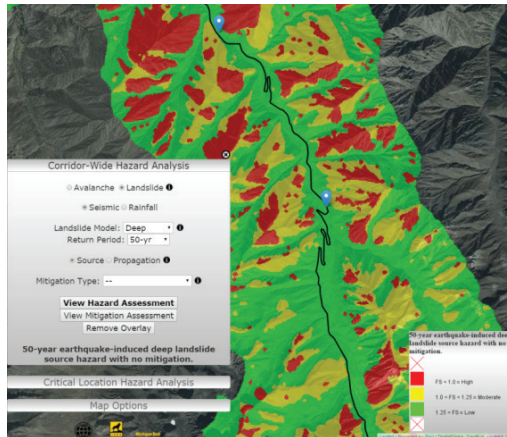
FIGURE 2. A SCREENSHOT OF THE DSS SHOWING EARTHQUAKE-INDUCED LANDSLIDE RISK AT THE CORRIDOR LEVEL.

Utilization of the best available landscape data coupled with a variety of geohazard modelling techniques enabled the production of hazard maps for multiple geohazard scenarios likely to occur in Afghanistan. The DSS parameters can be set for a variety of hazard types (shallow earthquake-induced landslides, deep

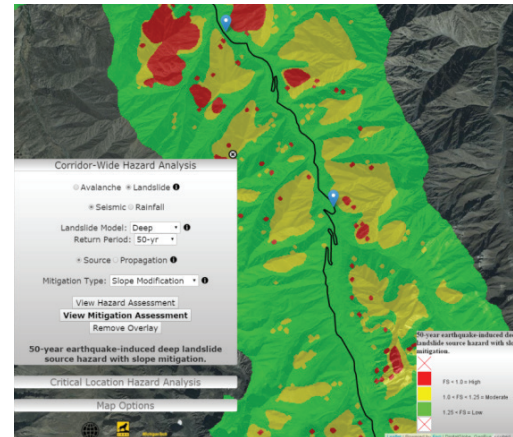
earthquake-induced landslide, rainfall-induced landslides) and return periods (10-year, 50-year, 100-year, 500-year, & 1000-year). For each hazard scenario, users can assess the change in hazard level with the implementation of the three mitigation strategies: slope modification, soil strength increase through mitigation measures such as

shortcrete, and ground water table reduction. Figure 3 shows the DSS with the 50-year deep earthquake-induced hazard assessment displayed, followed by the same assessment with each of the mitigation strategies implemented. Note that lowering groundwater or soil strength increase have minimal effect in this area considering the fact that the landslide is caused by earthquake. The slope modification mitigation is the most

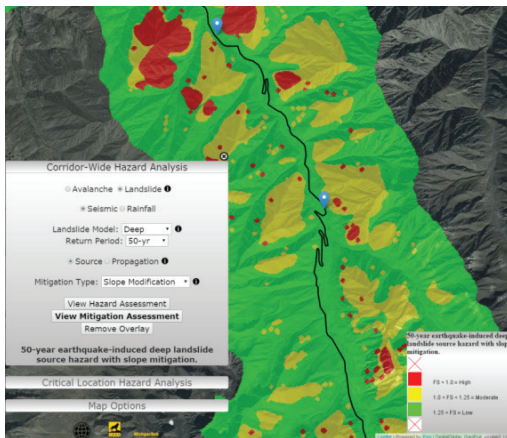
effective in risk reduction, but it also is the most costly to implement. This functionality will help transportation officials find an appropriate balance between cost and effectiveness when allocating resources to specific remediation efforts during the course of normal transportation corridor feasibility studies, detailed designs, and maintenance.



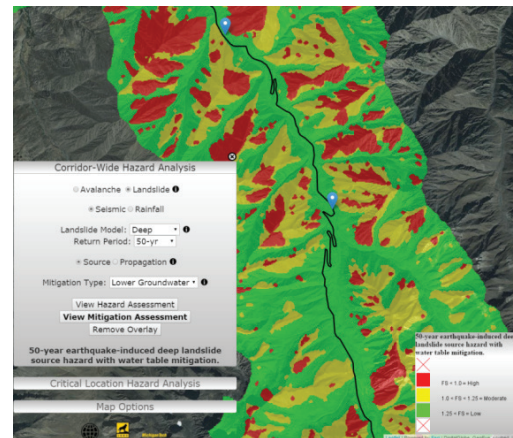
50-year deep seismic-induced hazard assessment (no mitigation)



50-year deep seismic-induced hazard assessment (Mitigation type: Soil strength increase)



50-year deep seismic-induced hazard assessment (Mitigation type: slope-modification)



50-year deep seismic-induced hazard assessment (Mitigation type: reducing groundwater level)

FIGURE 3. COMPARISONS OF HAZARD MAPS WITH THE APPLICATION OF THREE MITIGATION STRATEGIES.

High resolution digital elevation models (DEM) were used to calculate the hazard and mitigation along the corridor within the DSS. This enables users to view hazard assessments for specific localized areas of interest anywhere along the corridor, in addition to the corridor-wide scale in Figure 2. In Figure 4 the polygon outlined in blue is the area on both sides of the road that is affecting the location represented by the blue pin marker. This

region is approximately 5 square kilometers. In this way users are able to compute hazard zones for specific points anywhere along the road which can be added to the map interactively.

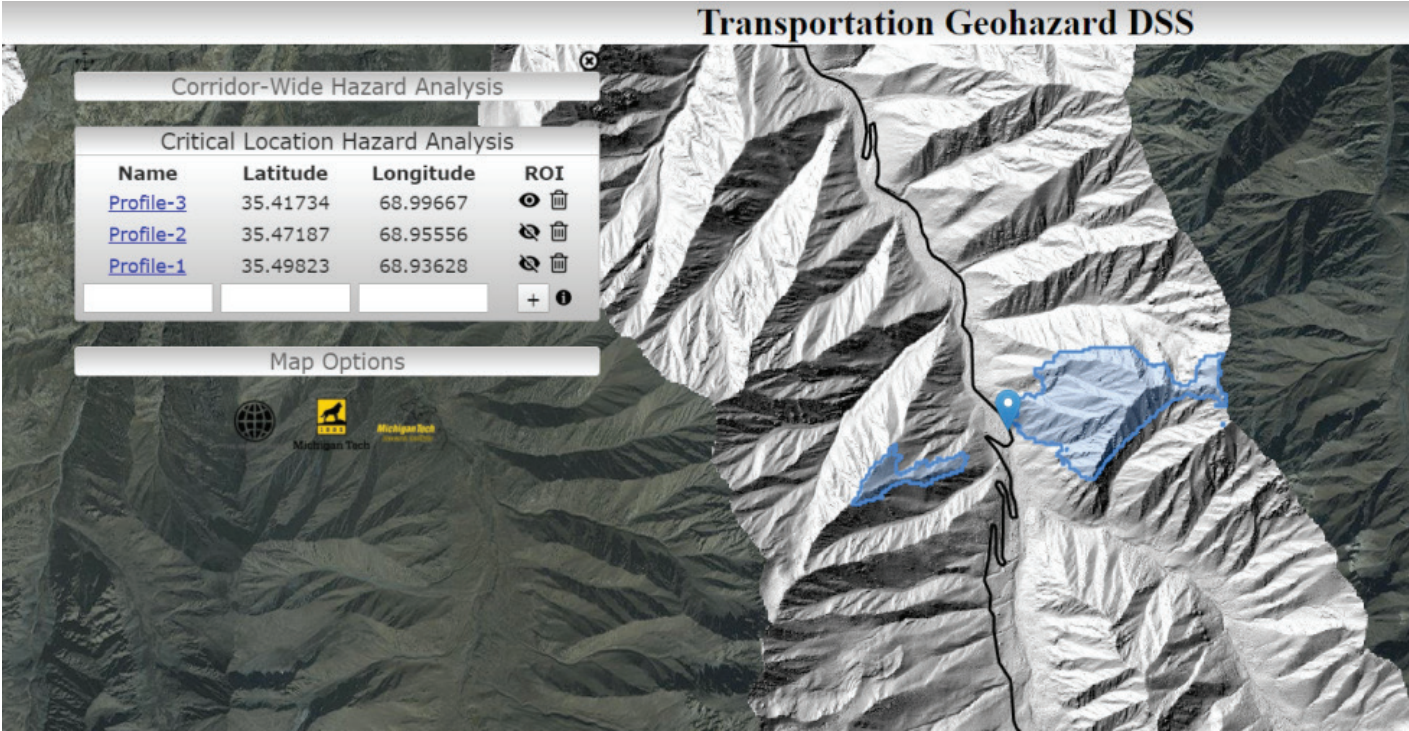


FIGURE 4. HAZARD ZONE CALCULATED FOR THE PROFILE-3 CRITICAL LOCATION

The DSS has the capacity of calculating a summary for the hazard severities within each local hazard zones. In the example provided in the Figure 5 below, 33% of the region is classified with high hazard pixels while 51% is moderate hazard and 15% is low hazard. At this location along the road over half of the area requires mitigation.

Selection and application of the various mitigation strategies will allow transportation officials to assess how those strategies will reduce risk. When slope modification is applied to the area in Figure 5, high hazard is reduced to 3% while moderate and low hazard areas have increased.

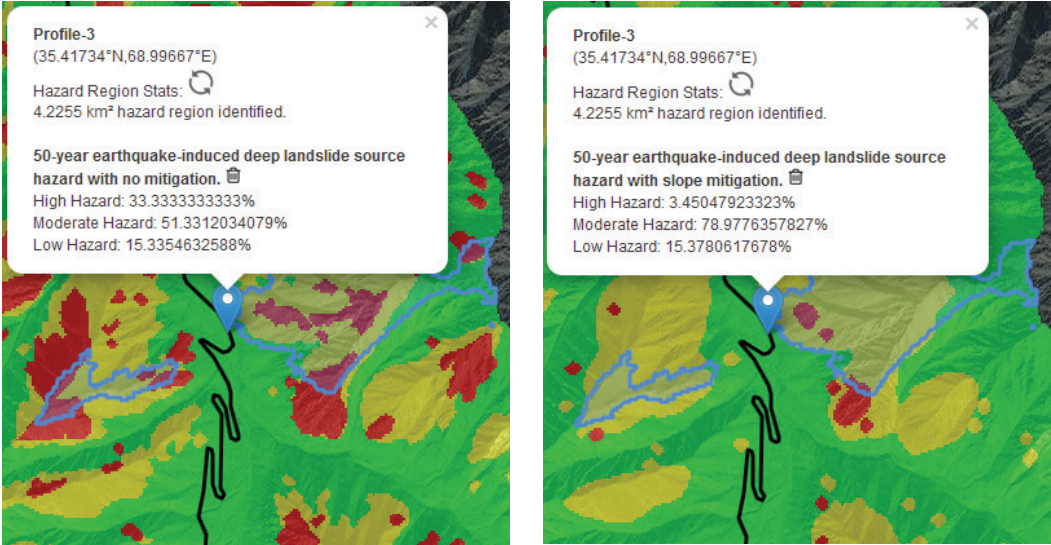


FIGURE 5. HAZARD ZONE SUMMARY CALCULATIONS FOR 50-YEAR EARTHQUAKE INDUCED LANDSLIDE WITH NO MITIGATION(LEFT) AND SLOPE MODIFICATION (RIGHT)

The DSS also has the capability to assess avalanche hazards. The avalanche assessment classifies each location within the transportation corridor in respect to the size of avalanche given a 100-year snowfall event. Figure 6 displays the avalanche risk for the entire transportation corridor. Note that extensive areas of the corridor, shown in green, have no avalanche threat at all. It should be noted, while useful for generalized planning purposes, the avalanche hazard assessment relies on modeled snowfall or actual snowfall calculations. Thus, in order for the DSS to be used as an

effective tool to plan for potential avalanche locations to provide emergency response, real-time meteorological data is required. A cost effective means of avalanche mitigation is to periodically reduce snow depth in avalanche prone areas through controlled explosions. This technique has been used effectively to manage avalanche risk in the western United States. The Colorado Department of Transportation reports using controlled explosions to trigger 283 avalanches in 2013-2014 (Colorado Department of Transportation 2017).

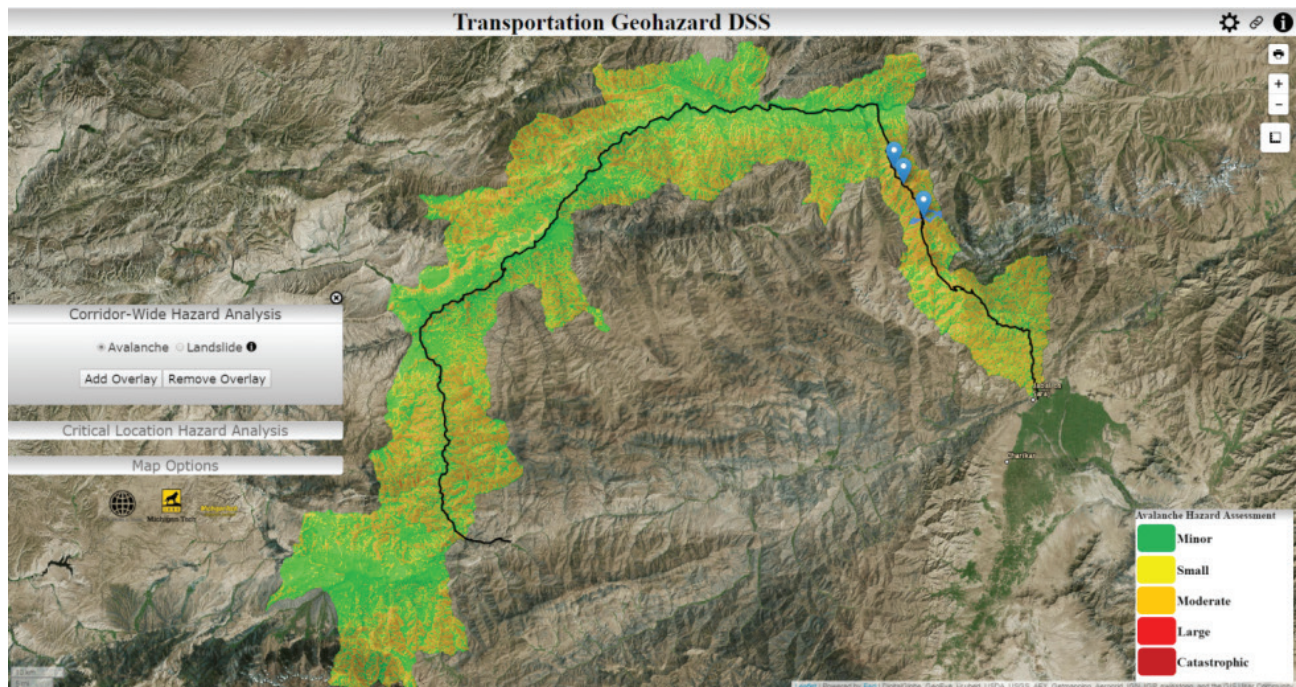


FIGURE 6. AVALANCHE HAZARD ASSESSMENT

The DSS has been developed to provide the functionality of a browser-based Geographic Information System (GIS). This enables users to perform GIS analysis from any computer, tablet, or smartphone with internet connectivity. The web architecture has been designed using open source software for the purpose of facilitating system integration with future or existing datasets and geospatial toolkits. An independent, portable server version of the DSS has also been developed to operate from a laptop which can be taken to the field or deployed in regions without wireless internet access. The DSS is also compatible with the Afghanistan GeoNode ([http://](http://disasterrisk.af.geonode.org/)

disasterrisk.af.geonode.org/), an online database of geospatial data in Afghanistan created by the World Bank.

Additionally, the DSS was developed to provide an intuitive interface for making informed engineering decisions based on sound scientific analysis. Rigorous hazard and mitigation models were employed with the highest quality available input data to ensure users can persistently rely upon the DSS as a relevant tool in the course of normal transportation management, from feasibility studies to detailed designs and maintenance.

2. User's Manual

Below is a detailed description of the specific hazard and mitigation assessments within the DSS, as well as a step by step description of the DSS's functionality.

2. A. LANDSLIDE ANALYSIS

Landslide hazard assessments were performed for shallow and deep landslides, and incorporate both seismic and rainfall triggers. Each landslide type was modelled for low, medium, and high return periods. For each permutation of landslide parameters, DSS hazard and mitigation assessments may be viewed according to the displacement quantity at the landslide source, or a factor of safety along the landslide propagation path (Figure 7). Geohazard assessments whose parameters share the same units were merged in combined hazard layers. To provide a synoptic overview, combined layers were also produced that merged the classified pixels, taking the highest risk level per pixel. These combinations include deep and shallow, and rainfall and earthquake landslide types. Altogether, the DSS contains 144 maps of modelled landslide risk.

Visualizing potential landslide hazard maps at the corridor-wide level is beneficial for determining generalized locations of where mitigation intervention is more likely to be needed. For example, West of Doshi there is 25 km of the highway corridor that is classified as "low hazard" (Figure 8) even during severe seismic or meteorological scenarios. Such an assessment enables transportation officials to focus their attention on other regions where hazard severity is higher.

Similarly, the user can select from several mitigation options. After users select which type of mitigation strategy they wish to apply, they can compare hazard levels along the transportation corridor both pre- and post-mitigation (Figure 9). The variety of hazard scenarios provides users with the ability to optimize available resources by focusing on areas that would benefit the most from mitigation techniques, given the geological and topographic conditions.

For a more detailed discussion of the modelling that was performed, refer to Section 6. Appendix. Landslide Hazard Modelling, Theory and Implementation.

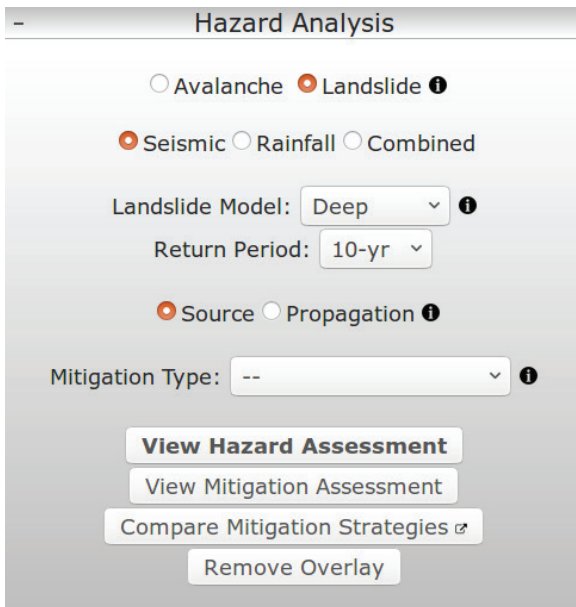


FIGURE 7. THE CORRIDOR-WIDE HAZARD ANALYSIS DASHBOARD MENU

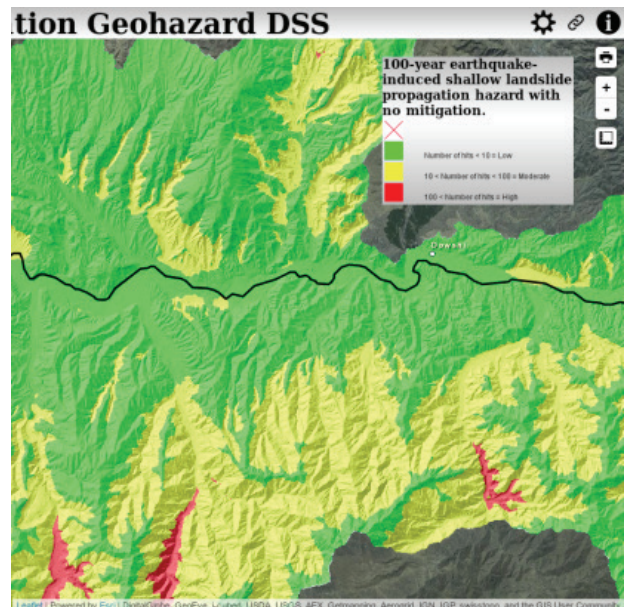


FIGURE 8. THE 100-YEAR RETURN EARTHQUAKE-INDUCED SHALLOW LANDSLIDE HAZARD WEST OF DOSHI

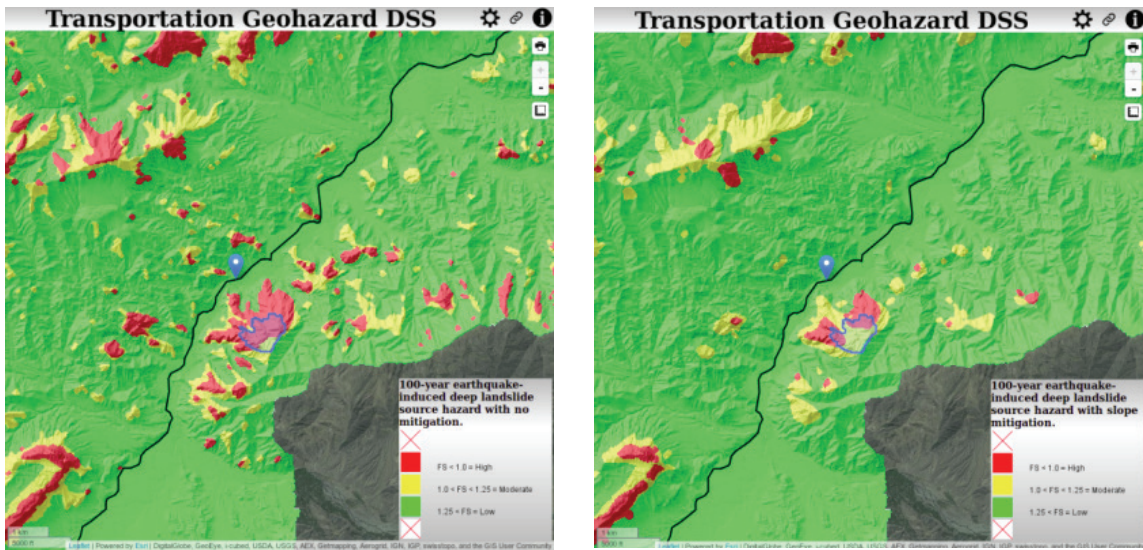


FIGURE 9. COMPARISON OF A REGION WITHOUT (LEFT) AND WITH MITIGATION (RIGHT).

2. B. AVALANCHE ANALYSIS

In addition to landslide hazards, users are able to view an analysis of avalanche hazards in the region. The avalanche assessment, completed for a previously completed World Bank funded effort, shows avalanche runout areas and

their associated avalanche pressure (in kPa) for a 100-year return period snow event. The results have been classified using a Canadian schema for classifying avalanche severity (Figure 10, McClung and Schaerer 1981).

Size	Destructive potential (definition)	Typical mass (t)	Typical path length (m)	Typical impact pressure (kPa)
1	Relatively harmless to people.	<10	10	1
2	Could bury, injure or kill a person.	10 ²	100	10
3	Could bury a car, destroy a small building*, or break a few trees.	10 ³	1000	100
4	Could destroy a railway car, large truck, several buildings or forest with an area up to 4 hectares (ha).	10 ⁴	2000	500
5	Largest snow avalanches known; could destroy a village or forest up to 40 ha.	10 ⁵	3000	1000

* e.g. a wood frame house

FIGURE 10. MCCLUNG AND SCHAEERER'S 1981 CLASSIFICATION SYSTEM FOR AVALANCHE SIZE.

3. Web DSS Interface

The Afghanistan Transportation Geohazard DSS is live on the web at <http://spatial.mtri.org/wbdss>.

This web interface provides a browser-based environment for viewing geohazard model assessments and comparing the effectiveness of modelled mitigation strategies.

The model data are organized using a Geoserver instance (<http://geoserver.org/>) that makes the data available as a WMS service which may be ingested by any web-enabled GIS (See section 3.c.).

The DSS web framework is served from an Apache server (<https://www.apache.org/>) located at Michigan Tech Research Institute in Ann Arbor, Michigan, USA. This server hosts all website source code and handles all the web traffic related to DSS access.

The DSS website is built around a Leaflet map viewer (<http://leafletjs.com/>) with a variety of HTML widgets that are driven by Javascript. Javascript must be enabled in web browser settings to use the DSS.

The DSS consists of two HTML templates: an overview window, and an analysis window. Each page's contents are customized to suit an analysis region. The following sections will cover each window's functionality in detail.

3. A. OVERVIEW WINDOW USER INTERFACE

The goal of the overview window is to provide a corridor-scale view of the risk assessment that was produced for this decision support system. Users may browse model results by toggling between hazard and mitigation assessments, zooming and panning around the region, and customizing their view of the data with various basemaps, ancillary datasets, and user annotations. The purpose of this design is to provide an intuitive web environment to contextualize hazard analysis raster layers with local geography, topology, and infrastructure. With this visualization of the local environment, project managers can better understand the extent of geohazards across the entire transportation corridor region.

The interactive regions in the DSS overview window are displayed in red in Figure 11.

- TOP BAR governs page functions.
- DASHBOARD governs map layer functions.
- LEGEND is populated when a geohazard layer is added to the map.
- Hovering the mouse over ⓘ will display tooltips containing user assistance and item descriptions. Clicking the ⓘ in the top bar will open a copy of this manual. When in doubt, consult the closest ⓘ

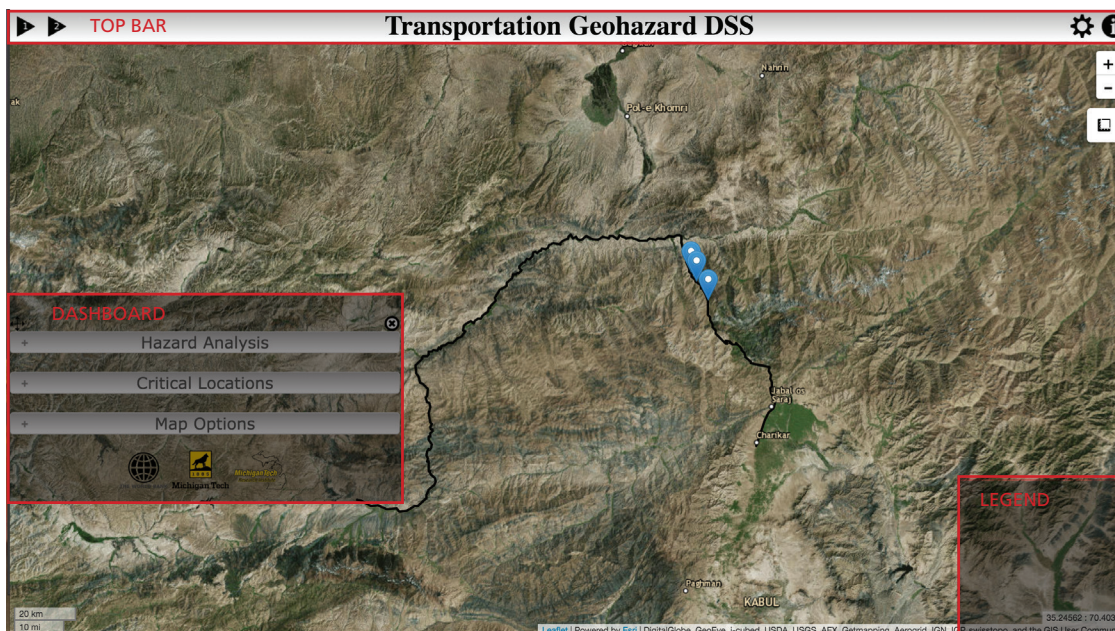


FIGURE 11. ANATOMY OF THE DSS OVERVIEW WINDOW.

3. a. i. Displaying Hazard and Mitigation Analyses

DSS map and layer functionality is provided through a dashboard interface.

The dashboard floats over the map and may be positioned anywhere by dragging it with the mouse. It can be hidden by clicking  and restored by clicking  in the top bar.

To display hazard and mitigation assessments, select the first dashboard section and identify the desired layer parameters. Figure 7 shows the parameters that users may add to the map. Selecting a layer from the dashboard will display the corridor-wide hazard or mitigation layer.

3. a. ii. Critical Location Assessment

Critical locations are named points of interest that can be added to the map viewer for geographic reference, or to compute the hazard areas directly threatening that point.

Users may drop custom pins anywhere on the map for reference. In the critical locations dashboard menu, enter a unique name and then either click the desired location

on the map, or enter known latitude and longitude coordinates (Figure 12). To delete a critical location, click .

Once a critical location is added to the DSS, it can be managed from the Critical Locations dashboard menu. In the Critical Locations dashboard menu, all critical locations are listed in a table format. The ROI column allows users to identify a region of interest that meets DSS criteria for geohazard threats. The DSS criteria identifies any area whose ratio of horizontal distance to vertical elevation exceeds a threshold value of 0.4 (Appendix 7, Figure 4). Slopes within the identified region of interest have a high likelihood of interfering with the critical location if they fail. Associating these regions of interest with areas that are classified as High- or Moderate-risk in the geohazard modelling can provide crucial information in supporting roadway management decisions.

Points at which detailed geohazard profiles have been drafted are preloaded on the map. Links to reports are contained in popups that are accessed by clicking their icon (). Geohazard regions of interest may also be requested from a critical location's popup dialog.



FIGURE 12. HAZARD ZONE CREATED ON THE FLY FOR A USER-DEFINED POINT ALONG THE CORRIDOR.

Once a critical location and region of interest are created, users may request a breakdown of the geohazard risk levels within the region of interest. If a region of interest is requested when a hazard or mitigation layer has already been added to the map then the statistics will be

displayed automatically. If a hazard or mitigation is added after the region of interest is computed, then the user will need to refresh the statistics from within the popup, by clicking . New statistics will be appended at the bottom of the popup, as shown in Figure 13.

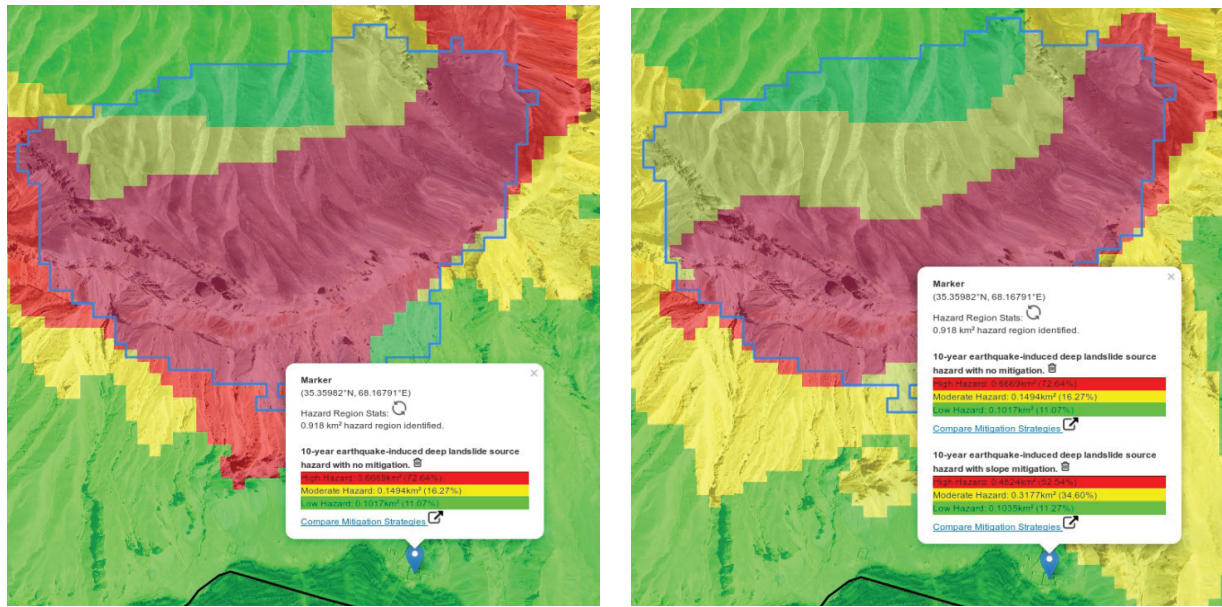


FIGURE 13. STATISTICS CALCULATED FOR A HAZARD ZONE FOR 10-YEAR EARTHQUAKE-INDUCED LANDSLIDES.

3. a. iii. Map Options

Users are offered various means to customize the map to suit their analysis.

Users have three options for basemap imagery: a composite of satellite and aerial ortho-imagery, a topographic hillshaded relief map, or a higher-resolution hillshaded DEM of the study area with no imagery displayed outside the study area.

The opacity of geohazard overlays may be adjusted via a slider in order to view basemap or ancillary data and provide context.

Buttons are provided to toggle ancillary data layers on/off. Ancillary data layers include the study area region, the corridor-wide hazard region of interest, line features of the study area roads, other regional roads and rivers, and a high-resolution (5 meter pixels) hillshaded DEM.

The study area region was designated to be restricted to all the watersheds through which the B2B and Salang Pass Highways pass through. Given that watersheds

3. B. ANALYSIS WINDOW USER INTERFACE

In contrast to the regional perspective provided by the overview window, the analysis window provides users with closer access to the data for the purpose of performing site-specific analysis. In the analysis window, users may

are delimited by the same surface drainage areas that landslides and avalanches follow, watersheds were used as the boundaries of the study area.

The study area road hazard area was produced by computing a geohazard region for every pixel along the study area road. Note that the geohazard region is identified by computing those regions whose ratio of horizontal distance to vertical elevation difference exceeds a threshold value of 0.4.

Users may add roadway buffers at 15, 25, 50, and 100 meters from the road to provide a sense of scale when viewing geohazard model results.

Local agencies use various roadway segmentation schema when viewing the road. Once such schema may be toggled on or off for the B2B Highway between Dushi and Bamyán.

Rivers, intersections, and other major traffic corridors in the study area region may be viewed by toggling the Ancillary Road Layer or Rivers Layer.

compare and quantify hazards, and understand the cost and related effectiveness of implementing mitigation strategies in specific locations.

The separate sections of the analysis window are displayed in red in Figure 14.

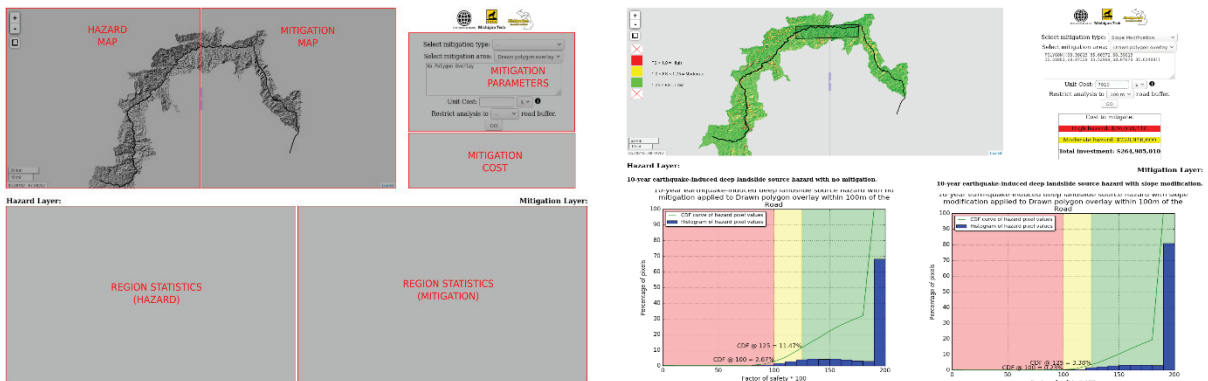


FIGURE 14. LEFT: ANATOMY OF THE DSS ANALYSIS WINDOW. RIGHT: A FULLY POPULATED ANALYSIS WINDOW.

3. b. i. Accessing the Analysis Window

The analysis window is accessed from the overview window in two ways:

1. When a hazard layer is added to the map, **Compare Mitigation Strategies** will appear in the hazard analysis dashboard menu. Clicking on this button will open the analysis window in a new tab.
2. When a critical location is selected, **Compare Mitigation Strategies** will appear in the critical location's popup as a button or hyperlinked text. Selecting this will open the analysis window in a new tab.

3. b. ii. Using the Analysis Window

The analysis window provides users with tools to identify and analyze specific hazard regions and mitigation sites in the study area region.

The analysis window's map viewer contains all the standard panning and zooming capabilities, and provides the study area DEM hillshade as a basemap. The map viewer also contains a slider, which allows users to view hazard and mitigation assessments side-by-side and to move the slider to change which assessment is shown in a given area.

The spatial analysis performed by the analysis window requires a region to be identified for analysis. This can be the hazard region computed in the overview window, or a drawn polygon overlay. If the analysis window was

accessed via the a critical location's popup (option 2 in Section 3. b. i.) and a geohazard region of interest has been computed for that critical location, then the region will appear in the analysis window's map. Alternatively, the measure tool in the analysis window's hazard map () can be used to draw a polygon for analysis. Please specify your choice in the "Select mitigation area:" drop down menu.

Mitigation layers may be added to the map by selecting a mitigation strategy from the "Select mitigation type:" drop down menu. This will also fill the "Unit Cost:" field with a default value to be used in estimating the cost for implementing the chosen mitigation strategy in the designated region. These default costs are \$US dollar amounts for known Afghanistan market values from May 2017. "Units" refer to 30 by 30 meter pixels used in geohazard modelling. Costing may be adjusted to match other known assessments.

Analysis can be further constrained to only consider a region within a certain fixed distance from the roadway. These fixed distances correspond to the DSS buffer distances of 15, 25, 50, and 100 meters. Selecting a buffer distance will display the roadway buffer in the map viewer.

Screenshots and downloads are encouraged in the analysis window. To download plots, right-click on the image and select the desired function to print. URLs to generated plots are not permanent, so exporting copies is the recommended method to archive and distribute DSS materials.

3. b. iii. Interpreting the Analysis Window Plots

The analysis window provides tools to quantify hazard and evaluate mitigation strategies in regions of interest. If there are values or figures that are of interest that are not directly provided by the DSS tools, those values and figures may still be interpreted from what is available.

For example, the overview window provides users with the area and proportion of each risk class within geohazard regions computed according to an algorithm described in Section 3. a. iii. If those area and proportion statistics are desired for a drawn polygon overlay in the analysis window, then those values may be calculated according to the following procedure:

1. First draw a polygon to indicate your region of interest and note the total area (848,830 square meters = .85 square km, see Figure 15). In this example, the following mountain top is used:

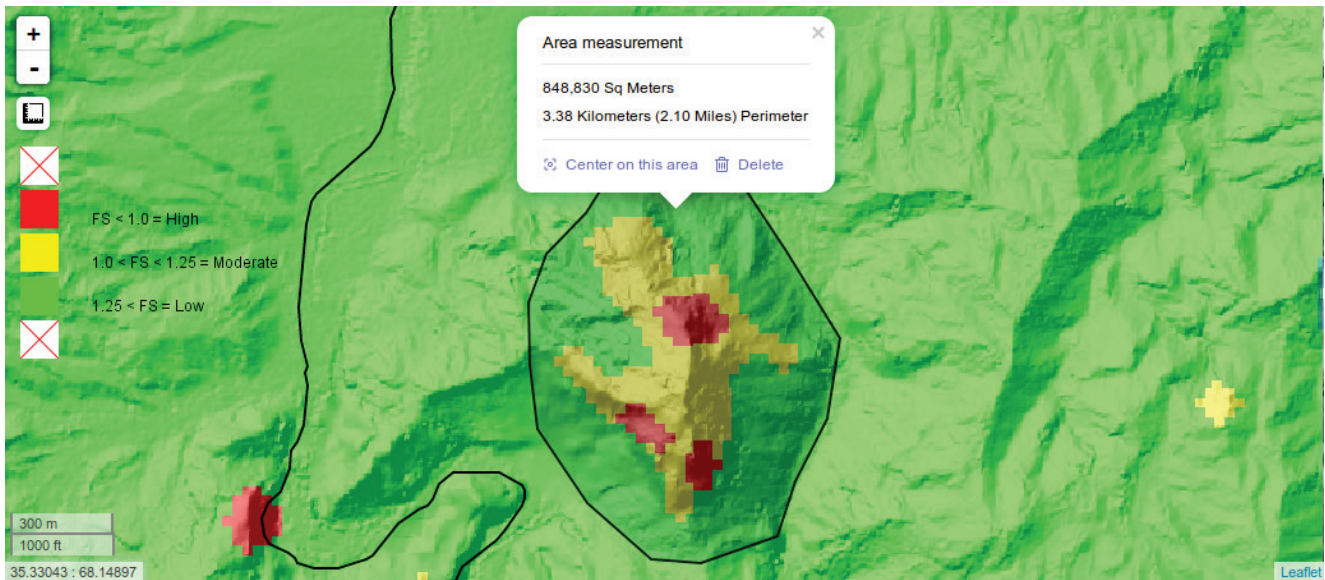


FIGURE 15. HAZARD LAYER WITH A MITIGATION AREA IDENTIFIED USING A DRAWN POLYGON OVERLAY.

2. Choosing slope modification as a mitigation strategy will display the mitigation assessment with a polygon indicating the designated region of interest (Figure 16):

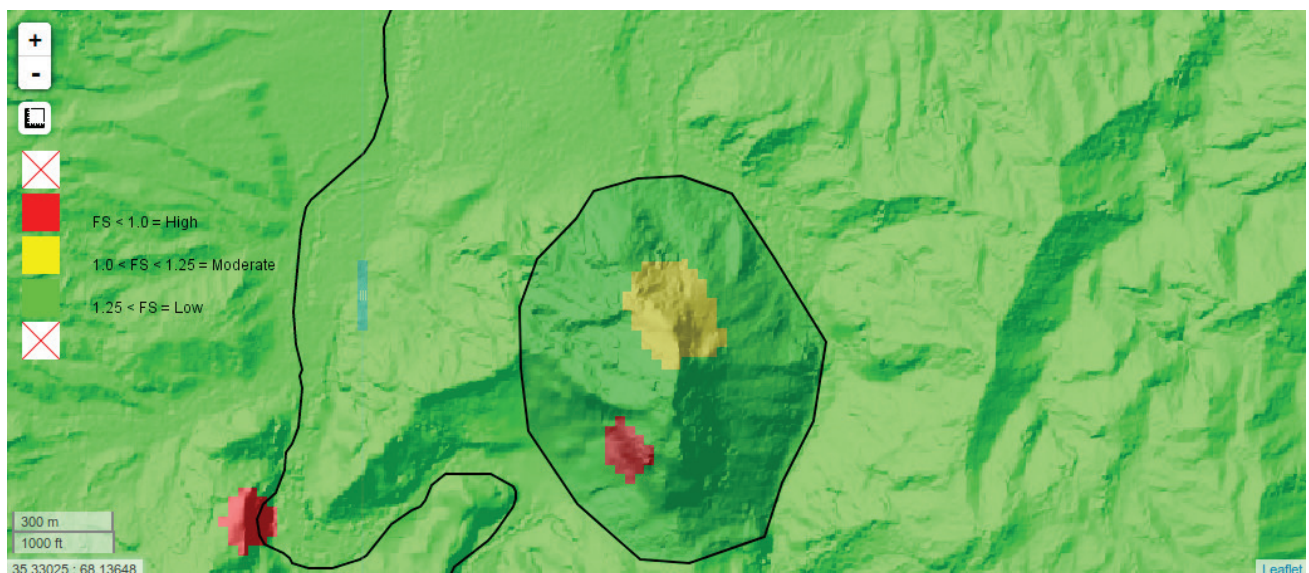


FIGURE 16. MITIGATION LAYER WITH A MITIGATION AREA IDENTIFIED USING A DRAWN POLYGON OVERLAY.

3. Clicking GO beneath the mitigation parameters will generate the following plots:

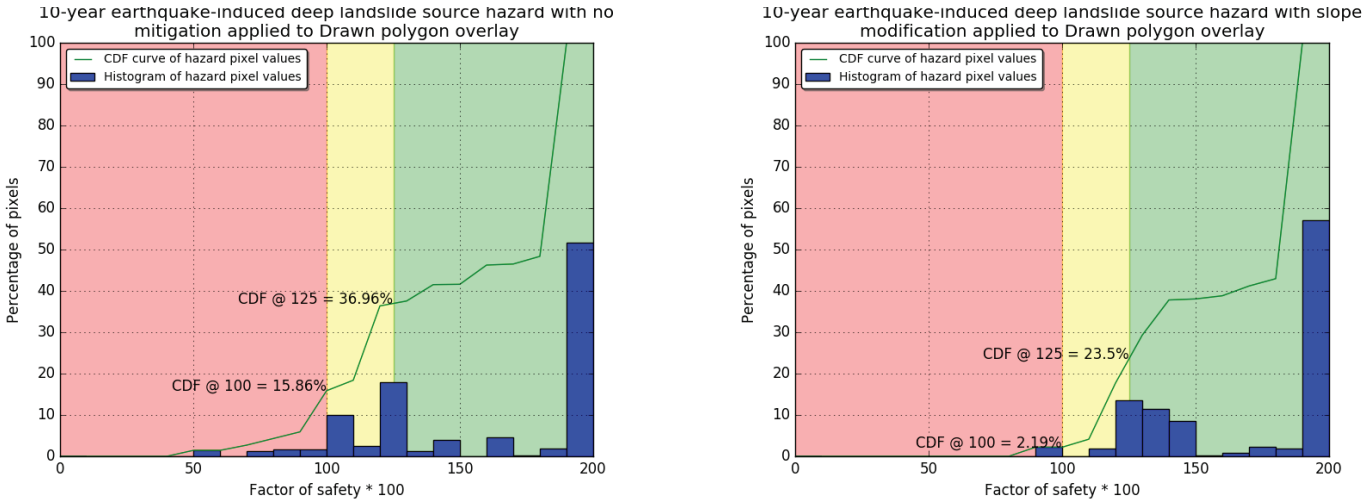


FIGURE 17. PIXEL STATISTICS FOR UNMITIGATED HAZARD (LEFT, FIGURE 15) AND MITIGATED HAZARD (RIGHT, FIGURE 16).

- 4. By looking at the CDF curve we can interpret the proportions. For the plot (Figure 17) with no mitigation applied on the left, 15.86% of the pixels are classified as High hazard, 21.1% (36.96-15.86 = 21.1) are Moderate hazard, and 48.18% are Low hazard. These can be multiplied by the total area to obtain values of 134,624 square meters for High hazard, 179,103 square meters for Moderate hazard, 408,966 square meters for Low hazard. For the plot with slope modification applied on the right, 2.19% of the pixels are classified as High hazard, 21.31% are Moderate hazard, and 76.9% are Low hazard. The total area for each hazard class in the mitigation assessment is therefore 18,589 square meters for High hazard, 180,885 square meters for Moderate hazard, and 652,750 square meters for Low hazard.
- 5. The unit cost can be applied to the total area to obtain a cost estimate for achieving this geohazard risk reduction. In this example, using the default slope modification cost value (US\$7010) across the entire mitigation area of 848,830 square meters (.85 square kilometers), would yield an estimate of US\$6,611,442.

3. C. WMS AND GIS INTEGRATION

Geohazard assessment data layers are stored using Geoserver software (<http://geoserver.org>), and may be viewed in web GIS environments.

To view DSS data layers in any internet-connected GIS, use the following as the WMS Server URL:

<http://geoserver2.mtri.org/geoserver/WBDSS/wms?request=GetCapabilities>

All model results and ancillary data products are persistently available via the above link as a WMS service.

4. Tutorials

4. A. INTERPRETATION OF THE FACTOR OF SAFETY

The factor of safety (Fs) is the ratio of resisting to destabilizing forces acting on a slope, such that when the Fs value is larger than 1 the slope is stable, and when the Fs value is less than 1 the slope is unstable (Chowdhury et al. 2010). Given the uncertainty in modeling results, it is commonly assumed that values of Fs above but close to 1 are not entirely stable but rather "marginally stable", and could become unstable if conditions changed slightly or the input data to the model were slightly inaccurate. It is common practice to consider the minimum acceptable factor of safety $FS = 1$ for pseudo-static seismic slope stability analysis, whereas a slightly larger minimum factor of safety (e. g. $FS = 1.25$) is used for other conditions, e. g. shear-friction method (e. g. Association of State Dam Safety Officials, 2017). For each modelling method applied the factor of safety can be interpreted in slightly different way, depending on the model reliability and the level of uncertainty in the model inputs.

For the precipitation triggered landslides, the modeled results include the estimated factor of safety at each location (pixel) in the area analyzed, as described in more detailed in the appendix and the references cited in it. The Fs values are highly sensitive to the inputs (e. g. Soil cohesion, friction angle, water table depth, water table depth, hydraulic conductivity, and hydraulic diffusivity) and can rapidly change in some cases, even if the input parameters only change slightly. For this reason we recommend using a minimum Fs value of 1.25 when considering what areas may be unstable, to account for the multiple, and probably interacting uncertainties in the modeling process.

The seismic triggered instability modeling is based on

standard limit equilibrium (e. g. extension of Bishop's method to three-dimensional cases) and Newmark displacement analyses (Chowdhury et al. 2010). The limit equilibrium analysis performed here for deep rotational slope failure considers worst case scenario input parameters (e. g. relatively low strength parameters) and we consider it's not necessary to be additionally cautious about the obtained Fs values. A similar rationale applies to the Newmark displacement analysis for shallow landslides triggered by earthquakes, particularly since we took a relatively conservative approach when converting the Newmark displacement values to equivalent Fs values; displacement values of only 5 and 15 cm where chosen for the limits between stable and marginally stable, and marginally stable and unstable classes, respectively, which in some cases (see Jibson et al., 2000) could correspond to only ~ 10 % and ~ 30 % probability of failure. For these reasons, we recommend using a minimum Fs value of 1 when considering what areas may be unstable.

4. B. DETERMINE AN OPTIMAL MITIGATION STRATEGY

This section describes a typical use case for the determination of the optimal mitigation strategy to implement at a specific location (Figure 18).

This demonstration will focus on the intersection of the Barfak-Bamiyan Highway with the Bamiyan-Charikar Highway, and the susceptibility of this location to geohazards that may result from a 10-year seismic event.

Once the DSS is open in a web browser, enter the intersection as a critical location as described in section 3.b. Both highways may be viewed by toggling the study area road and ancillary roads layers, or viewing the aerial imagery basemap in the Map Options menu:



FIGURE 18. A CUSTOM CRITICAL LOCATION ADDED TO THE OVERVIEW WINDOW.

To compute the region that contains geohazards that threaten this specific location, select the Compute Hazard Zone button in the popup window that describes that critical location. A high resolution DEM may be displayed

in the Map Options menu, such as shown in Figure 19, but this is only a visual aid for users and is not necessary to perform the computation.

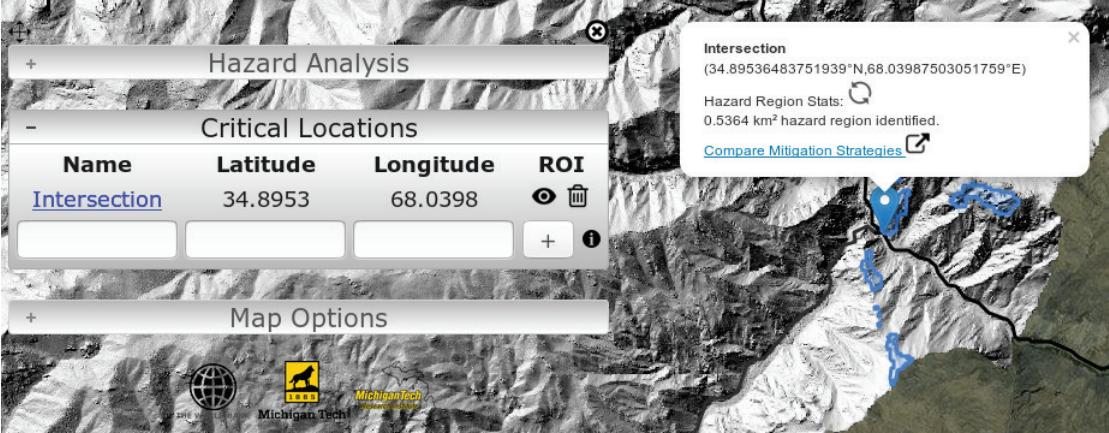


FIGURE 19. A HAZARD REGION GENERATED BY THE DSS AT A CUSTOM CRITICAL LOCATION.

Note that the visibility of the region of interest for this critical location may be toggled from the Critical Locations menu. This may be useful to distinguish multiple proximate critical locations' hazard regions.

To analyze the geohazard for this area, enter the hazard conditions in the Hazard Analysis menu (Figure 20):

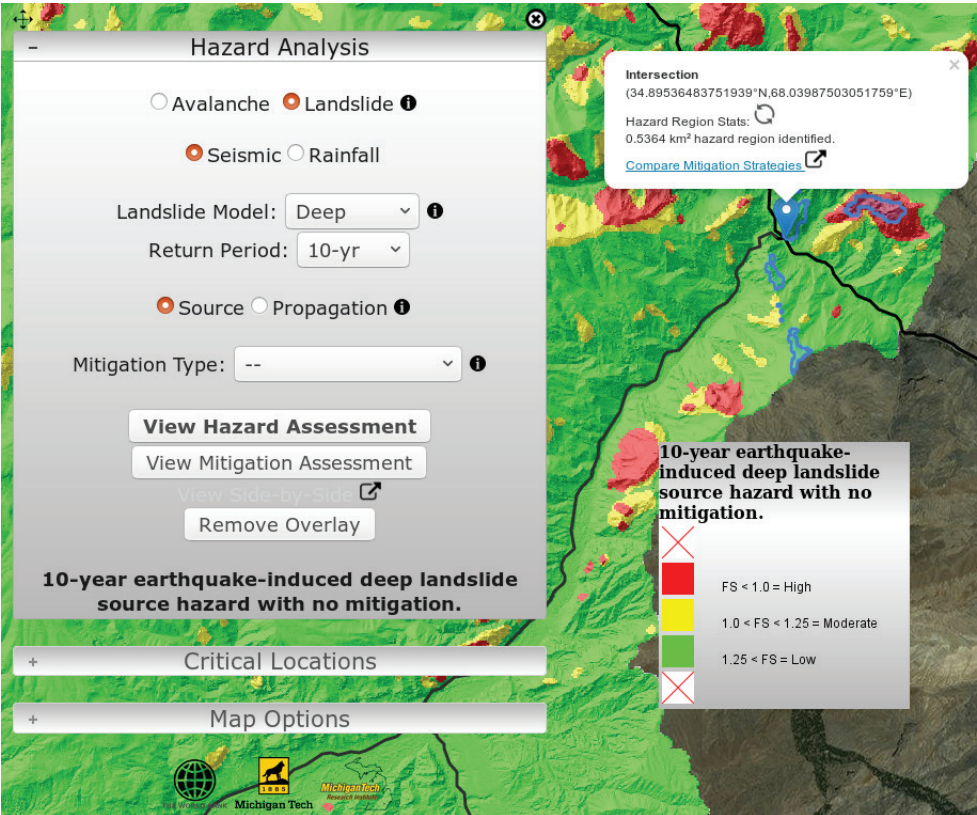
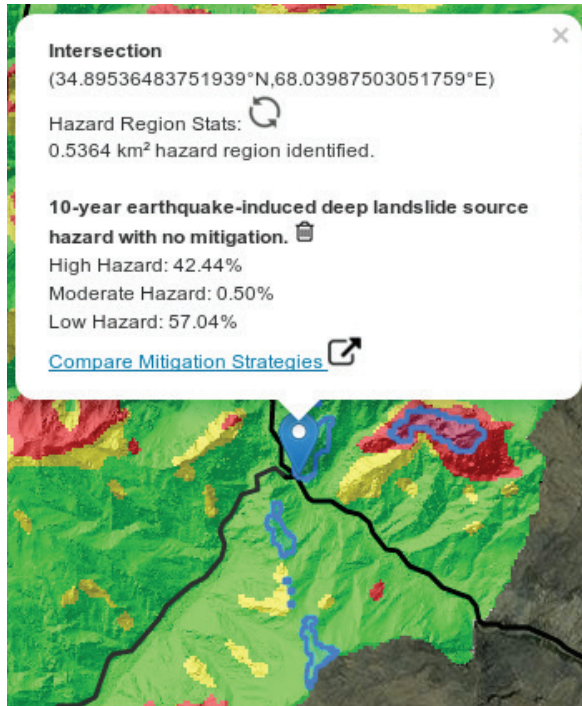


FIGURE 20. AN UNMITIGATED HAZARD LAYER SHOWN WITH A CUSTOM CRITICAL LOCATION AND HAZARD REGION GENERATED BY THE DSS IN THE OVERVIEW WINDOW.

To view a summary of the hazard levels in the region identified as posing a threat to the highway intersection,



refresh the hazard region statistics in the popup window (Figure 21):

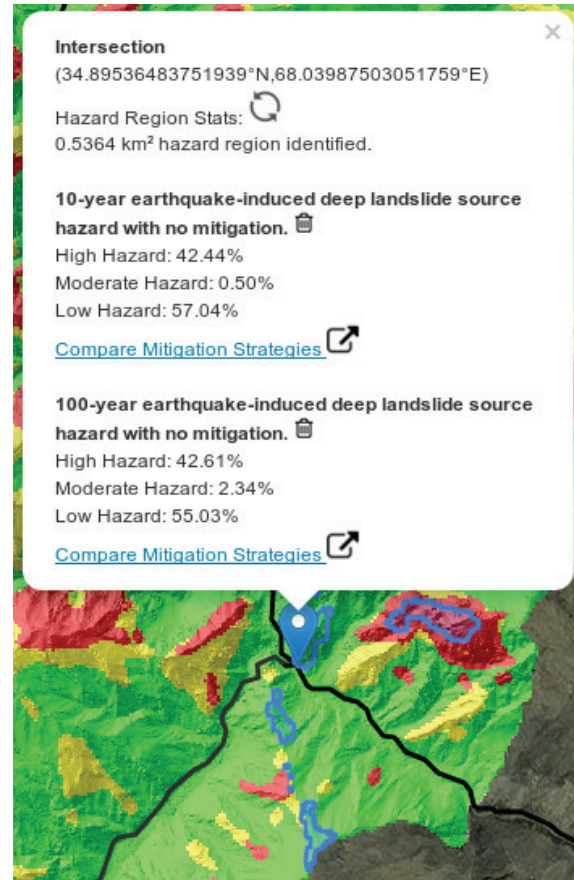


FIGURE 21. PIXEL STATISTICS FOR THE HAZARD REGION IDENTIFIED AT A CUSTOM CRITICAL LOCATION. WHEN A NEW HAZARD LAYER IS SELECTED, NEW PIXEL STATISTICS ARE APPENDED TO THE POPUP (LEFT).

Note that adding a new hazard or mitigation assessment layer will allow users to refresh the summary statistics in the popup window. New summary statistics will be appended to the popup window, so that users can make preliminary comparisons between hazard conditions and mitigation assessments. In this example, the difference between 10-year and 100-year seismic events is minor.

To determine the optimal mitigation strategy to reduce the geohazard risk at this location, click the Compare Mitigation Strategies link below the summary statistics for the particular geohazard assessment to be mitigated. This will open a new window.

In this new window, the hazard assessment is displayed on the left, and mitigation assessments will be displayed on the right. A plot on the left is generated that displays a histogram and cumulative density distribution of the

actual numeric geohazard magnitudes in the region identified by the DSS (Figure 22). This demonstrates the severity of risk within the region more precisely than the low/moderate/high classification provided in the previous corridor-wide view.

On the right, there is a drop-down menu that allows users to select between mitigation strategies whose effectiveness has been modeled using the specified conditions. Once the user selects a mitigation assessment, the data is displayed on the right side of the map viewer at the top of the page under a slider that users may slide back and forth, comparing the hazard and mitigation assessments. The histogram and cumulative density distribution for the mitigation layer will also be plotted for the mitigation layer's data, below the map viewer, and to the right of the hazard data plot.

The figure 22 shows the material generated when slope modification is applied to these hazard conditions.

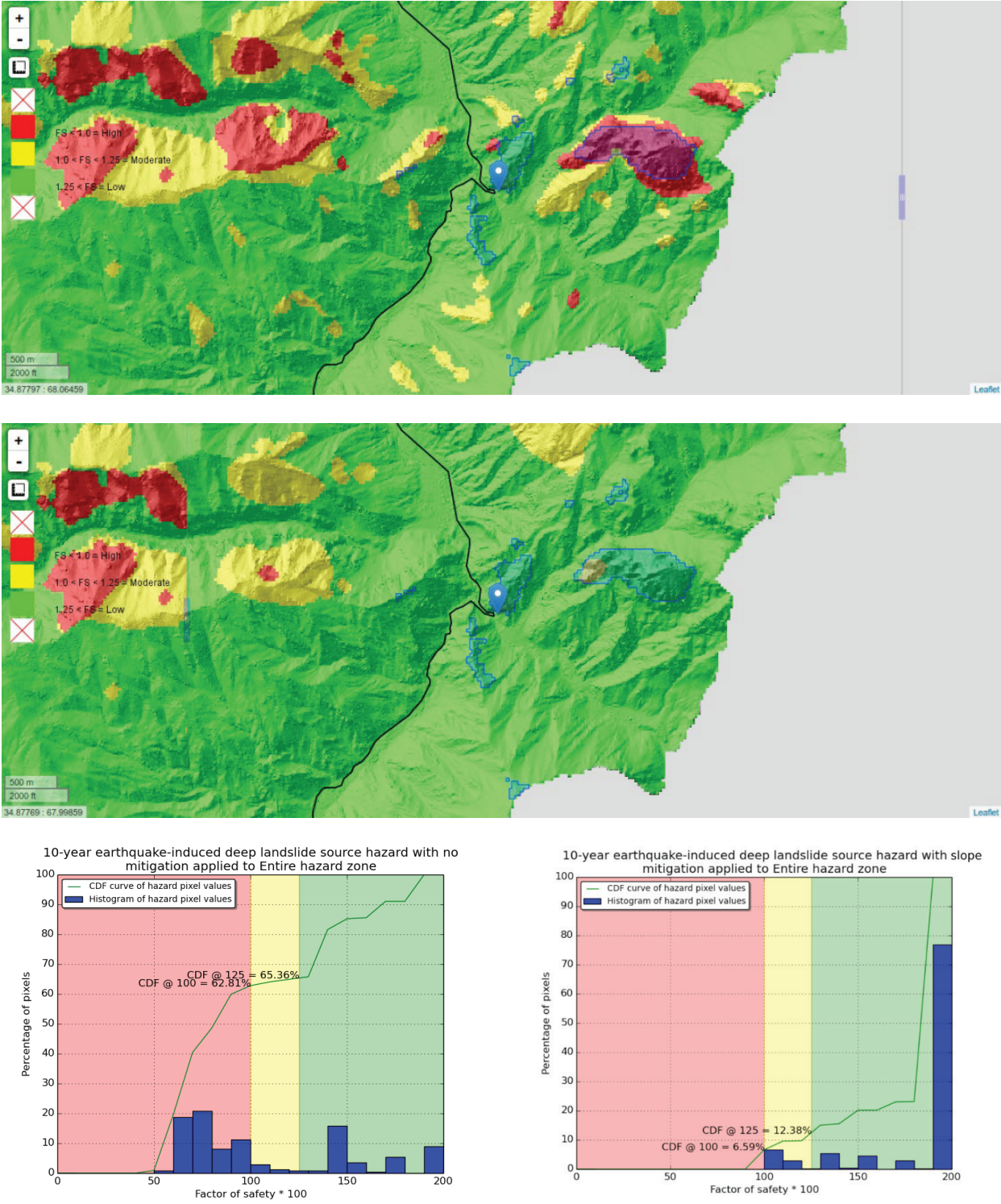


FIGURE 22. FIGURES GENERATED BY THE ANALYSIS WINDOW. TOP MAP SHOWS UNMITIGATED HAZARD ANALYSIS, BOTTOM MAP SHOWS SLOPE MITIGATED HAZARD ANALYSIS. LEFT PLOT SHOWS UNMITIGATED PIXEL STATS, RIGHT PLOT SHOWS PIXEL STATS ONCE SLOPE MODIFICATION HAS BEEN IMPLEMENTED.

4. C. INTEGRATING MODEL RESULTS WITH GEONODE

The World Bank Group has collected several national datasets for Afghanistan that have been made available at <http://disasterrisk.af.geonode.org/>. As of June 2017,

GeoNode contains 93 unique geospatial datasets that comprise 11 maps that are used in regional analyses of various disaster risks.

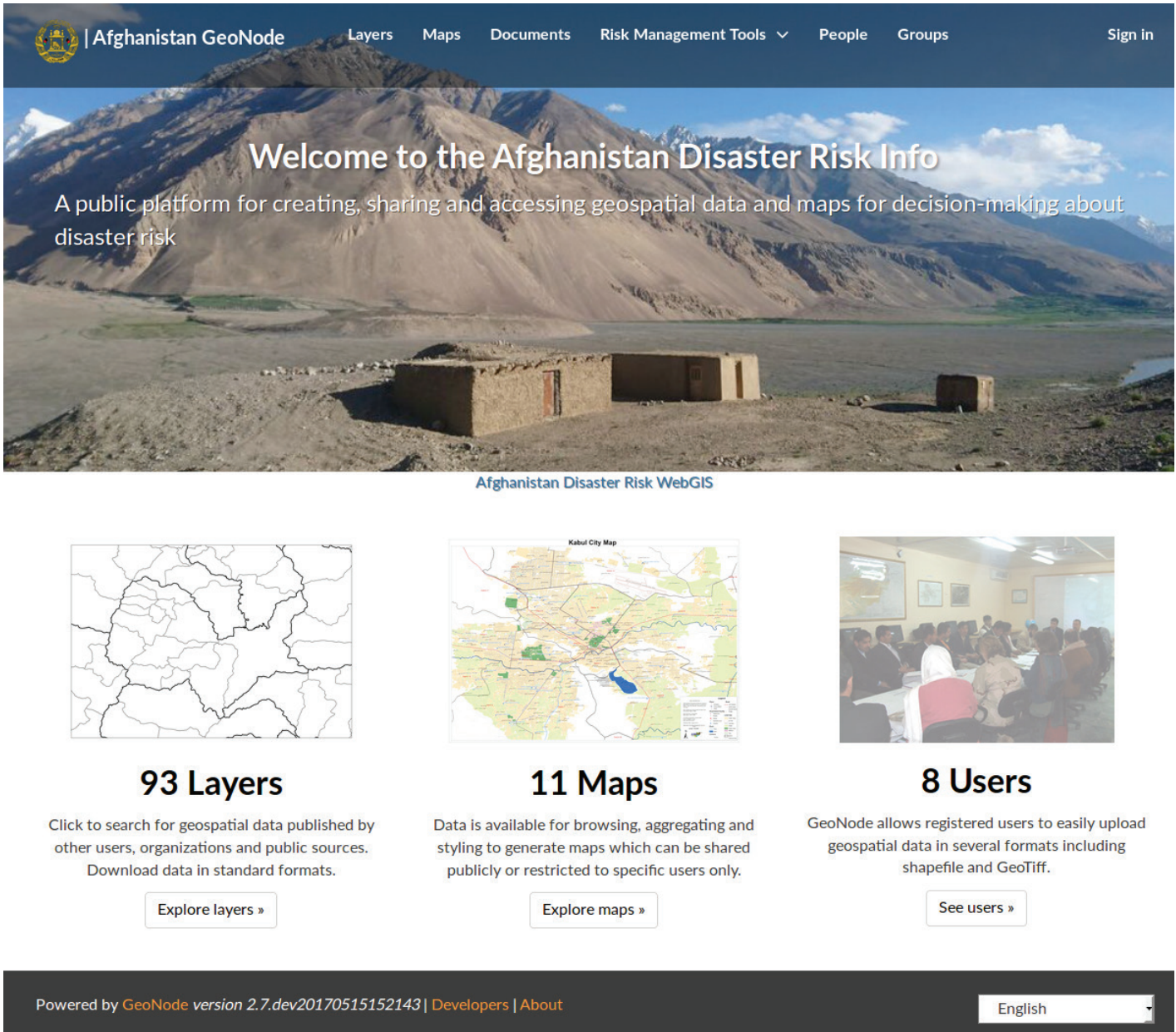


FIGURE 23. GEONODE LANDING PAGE.

Model results that are used in the DSS may also be viewed in GeoNode maps. For example, figure 23 displays the GeoNode map for "Schools, landslides, and floods," which consists of geohazard assessments of flood hazard

and landslide susceptibility, overlaid with national data representing the locations and sizes of universities, high schools, secondary schools, and primary schools.

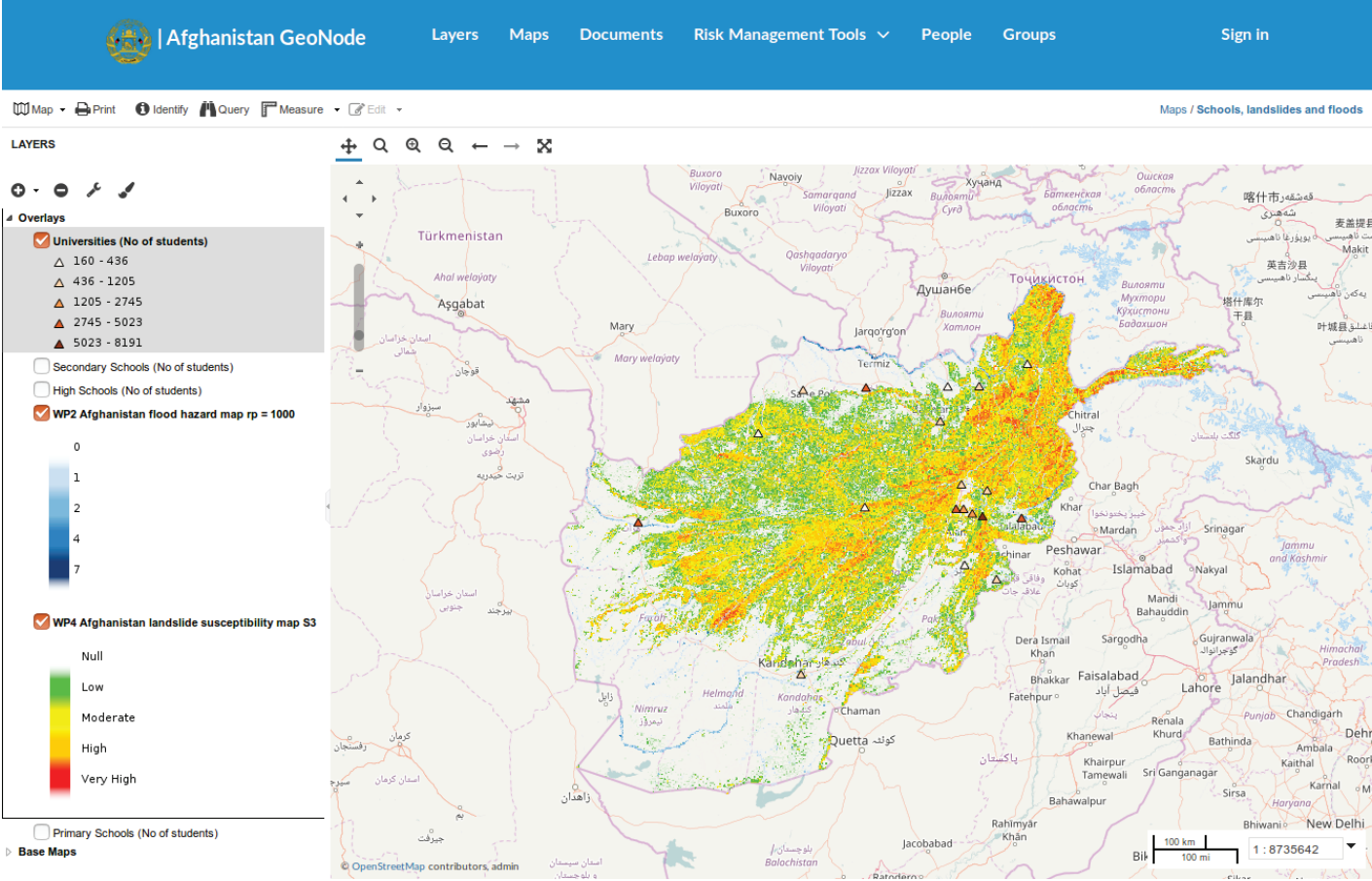


FIGURE 24. GEONODE MAP FOR SCHOOLS, LANDSLIDES, AND FLOODS, DISPLAYING UNIVERSITIES AND BOTH RISK ASSESSMENTS.

To add DSS modelling products to GeoNode maps, we will be using the WMS service described in section 3. c.

Clicking in the top left of the window allows users to "Add layers". In the drop-down menu that appears, select "Add a new server...". Ensure the server "Type" is "Web Map Service (WMS)", and enter the DSS model results' WMS URL:

<http://geoserver2.mtri.org/geoserver/WBDSS/wms?request=GetCapabilities>

Once the WMS URL is entered, clicking will show a list of all the layers available to be used as hazard layers, mitigation layers, or ancillary data layers in the DSS.

5. Troubleshooting

If problems are encountered that are not resolved by referring to the table below, please contact Sam Aden <staden@mtu.edu>. Thank you for working with Michigan Tech.

PROBLEM	SOLUTION
Buggy behavior previously encountered.	Refresh DSS page (Ctrl+F5)
Dashboard - Map layer mismatch	Remove & re-add layer
Hazard or ancillary vector overlays not scaling with zoom level	Refresh DSS page (Ctrl+F5)
Floating dashboard or legend placement is restricted	Set window to desired size and refresh DSS page
Analysis window plots do not correspond to the region identified.	Click "GO" again to regenerate plots.
404 Not Found / Server Timeout	Try again later or notify Sam Aden <staden@mtu.edu>

6. Appendix. Landslide hazard modeling: theory and implementation.

6.A. MODELS AND THEORETICAL BACKGROUND.

Landslide hazard was assessed for a variety of potential future hazard conditions. Although landslides can happen independently of the occurrence of any obvious triggers, most landslides are triggered by external environmental factors. Our initial assessment of the conditions for the B2B and Salang Pass roads suggested that two main processes may be the main landslides triggers in the area: water infiltration in the soil due to precipitation (as both rainfall and, snow and ice water melting), and ground shaking due to earthquakes. A variety of landslide mechanisms and types have been established (Hung et al. 2014 and references therein), but here we consider

only two main types of landslides that we estimate cover most cases that we would expect to encounter in the terrain being analyzed: shallow translation landslides, and deep rotational landslides. Assessing the landslide hazard involves determining the areas that could potentially become unstable, and if such instabilities occurred, how far would the sliding material move. Therefore, two processes associated with the hazard need to be assessed, the sources process and the propagation process (see Figure 25).

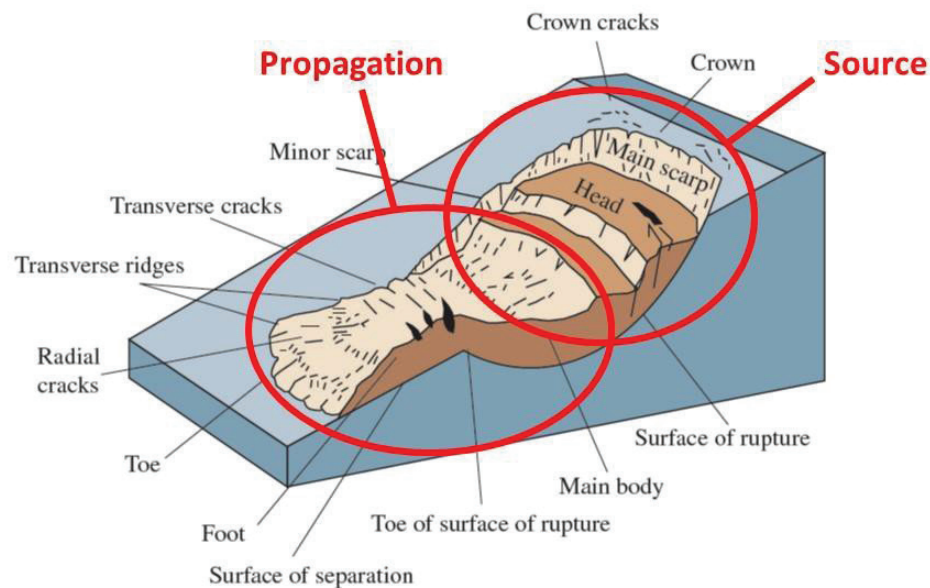


FIGURE 25. ILLUSTRATION OF SOURCE AND PROPAGATION (RUNOUT) OF LANDSLIDES.
MODIFIED FROM [HTTP://PUBS.USGS.GOV/FS/2004/3072/PDF/FS2004-3072.PDF](http://pubs.usgs.gov/fs/2004/3072/pdf/fs2004-3072.pdf)

The first step in assessing the landslides hazard was to model the conditions that would lead to slope instability and landslide initiation. In shallow landslides the unstable portion of the slope is confined to a zone close to surface and it is usually assumed that its geometry is rather simple (the failure surface extends parallel to the surface). Our models for this type of instability are based on the "infinite slope" (see figure 26) concept (Chowdhury et al. 2010), modified for rainfall induced landslides (Baum et al, 2002) and earthquake triggered landslides (Jibson, 2007). For shallow landslides triggered by precipitation the TRIGRS model was used (Baum et al, 2002), shallow

landslides triggered by earthquakes were modeled with the Newmark displacement method (Jibson, 2007), and deep landslides triggered by earthquakes were modeled with the Scoops3D model (Reid et al. 2015). The triggering of deep rotational landslides by water infiltration is less common, but is also less well understood, in this work we did not directly account for such cases in our modeling. The inclusion of the other cases should in any case be extensive enough that areas that could potentially fail as deep landslides triggered by water infiltration are for the most cases already covered by the other cases.

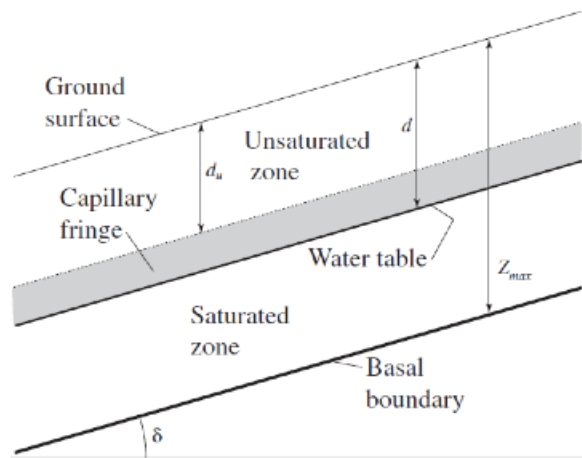


FIGURE 26. ILLUSTRATION OF THE INFINITE SLOPE MODEL FOR LANDSLIDES. MODIFIED FROM USGS [HTTPS://PUBS.USGS.GOV/OF/2008/1159/DOWNLOADS/PDF/OF08-1159.PDF](https://pubs.usgs.gov/of/2008/1159/downloads/pdf/of08-1159.pdf)

In deep landslides the unstable portion of the slope can extend further down and have a much more complex geometry. Our models are based on the three dimensional rotational landslide model (Reid et al. 2015) (see Figure 27).

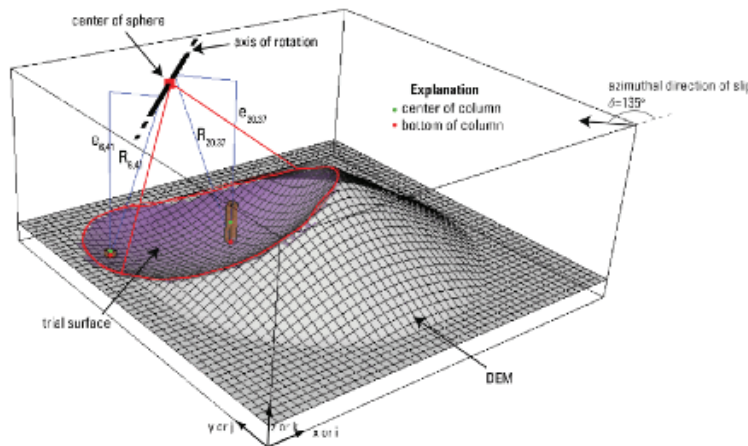


FIGURE 27. ILLUSTRATION OF THE THREE-DIMENSIONAL ROTATIONAL MODEL FOR LANDSLIDES. MODIFIED FROM USGS [HTTPS://PUBS.USGS.GOV/TM/14/A01/PDF/TM14-A1.PDF](https://pubs.usgs.gov/tm/14/a01/pdf/tm14-a1.pdf)

After the source area for a landslide has become unstable, the landslide mass moves downslope, potentially reaching areas where population and infrastructure may be exposed. Therefore, additionally to the generation of the landslide by slope instability processes it is also necessary to assess the landslide mass propagation process, to evaluate what areas may be exposed to the hazard. To model the propagation the height to length concept, also known as energy line (or cone, in three dimensions) was used (Hunter and Fell, 2003; Finlay et al. 1999).

Models assess slope stability through the infinite slope model for shallow translational landslides, and by the Bishop circular failure models for deep rotational landslides. Water infiltration (rainfall and snowmelt) triggered landslides is modeled in detail using the TRIGRS software published by Baum et al. (2009) from the United States Geological Survey (USGS), which combines the infinite slope model with saturated (suction reduction) and non-saturated (pore pressure increase) reduction of soil strength in response to the water infiltration. This model predicts the factor of safety of points on the landscape subject to a given rainfall intensity and duration (Baum et al. 2002).

The seismic ground motion triggering effect was modeled through pseudo-static analysis incorporating Newmark displacement analysis for critical peak ground acceleration (PGA) levels. For shallow slopes we use the infinite slope model, coupled with a Newmark seismic displacement model (Jibson, 2007), which considers the stability of the slope in terms of the slope deformation. The output of the model is not an F_s value, but a deformation, to make this deformation compatible with other hazard assessment outputs we converted the displacement values to equivalent F_s . For the deep seismic triggered landslide modeling we used the SCOOPS3D computer program published by the United States Geological Survey (USGS) (Reid et al. 2015), which outputs results as F_s value maps.

Selection of infiltration (from rainfall and snowmelt) events scenarios and probabilities was guided by the prior analysis on flooding hazard, which will also allow for consistency of our work with the results from previous work components. The database on rainfall events compiled for the GeoNode portal was used for this analysis for five return periods: 10, 50, 100, 500, and 1000 years. Ground shaking intensities (PGA) from the same source and for the same return periods was also used.

The potential propagation of the landslides was assessed considering the height to runout ratio approach (Hunter and Fell, 2003; Finlay et al. 1999). This approach considers how far a landslide mass will reach from its source location, by taking into account how much elevation it loses along its trajectory. This roughly corresponds with the physical concepts of driving energy, i.e. the potential gravitational energy that allows the landslide to move in the first place (represented by the elevation drop), and resistive frictional energy, i.e. the energy dissipation that the landslide mass experiences as it moves along its trajectory (represented by the distance traveled). The ratio between the height drop (H) and runout distance (L), H/L then becomes a measure of the landslide's mobility that can be applied to different topographic settings. Although limited in many aspects, this mobility measure is relatively easy to evaluate, as it only depends on the topography, and it has been found that it correlates with the landslide volume. For our analysis purpose we used a constant value for the H/L ratio of 0.4, representing typical landslides in the range of 10⁴ – 10⁵ m³, a range of values expected to be an average for landslides in the analyzed area.

6.B. MODEL INPUTS AND DATA.

The input data for the models used in our analysis include data on topography, soil and rock properties, and potential triggering events (rainfall and earthquakes). Topography was represented through digital elevation models (DEMs) from which slope inclination values used in the shallow landslide models were derived. Analyses were performed on DEMs of different resolutions, mainly a 5 m resolution local DEM for Afghanistan, and the 30 m resolution SRTM DEM (USGS, 2017). The final aggregated results are presented in the 30 m resolution to precisely represent the limiting resolution in our analysis.

Physical processes based models for slope stability analysis require the strength properties of the slope materials as an input into the model. Commonly the materials' strength is characterized through the internal friction angle (ϕ) and the cohesion (c). These values are usually obtained from laboratory tests on samples of slope material, but can also be estimated from proxies in the field. In this case, soil and rock properties (strength parameters, densities and weights, grain size distributions) were based on a sample of geotechnical testing data provided by the Afghan counterparts for a limited number of sampling sites along the B2B road. Other material physical parameters

used by the models (e. g. rock, soil and regolith unit weights) are less critical to know with precision and were estimated from the same geotechnical reports.

Knowing the hydrologic properties (such as diffusivity, saturated conductivity, etc.) of the slope materials is also necessary for applying the models we used. Such properties were derived based on grainsize distribution and its relationship to geotechnical properties. Estimates of the water table level for some wells in the area have been reported by the USGS (Mack et al. 2014). A global water table model was also used (Fan and Miguez-Macho, 2013) and refined to a higher resolution to match the resolution of the other datasets, using the height above drainage concept (Nobre et al, 2011). Similarly, a global dataset on soil and regolith (Pelletier et al., 2016) depth was used and refined using a correlation with terrain slope.

The same models were used with modified input parameters to simulate the effect of different mitigation strategies. Slope terrain modification was modeled

by representing terrain with lower slope values in all models, but only for the highest slope values. The lower slope terrain model was used for input in all modelling programs, with all other input parameters held constant, to evaluate the effect on the model outputs, and take those differences as the terrain performance improvement under the landslide triggering conditions. In practice a similar effect could be attained through cut-and-fill techniques of the potentially unstable slopes, complemented by some minor retaining structures and erosion control measures. A similar approach was used to model the effect of increasing the soil strength, changing the value of cohesion in the inputs for the models. The increase in cohesion could be equivalent to the effect that some simple slope stabilization techniques could have (e. g. minor retaining structures and erosion control measures). In the case of drainage improvement, the effect was modeled by accounting for a deepening of the water table, as such could be the effect of improving the drainage on the slopes.

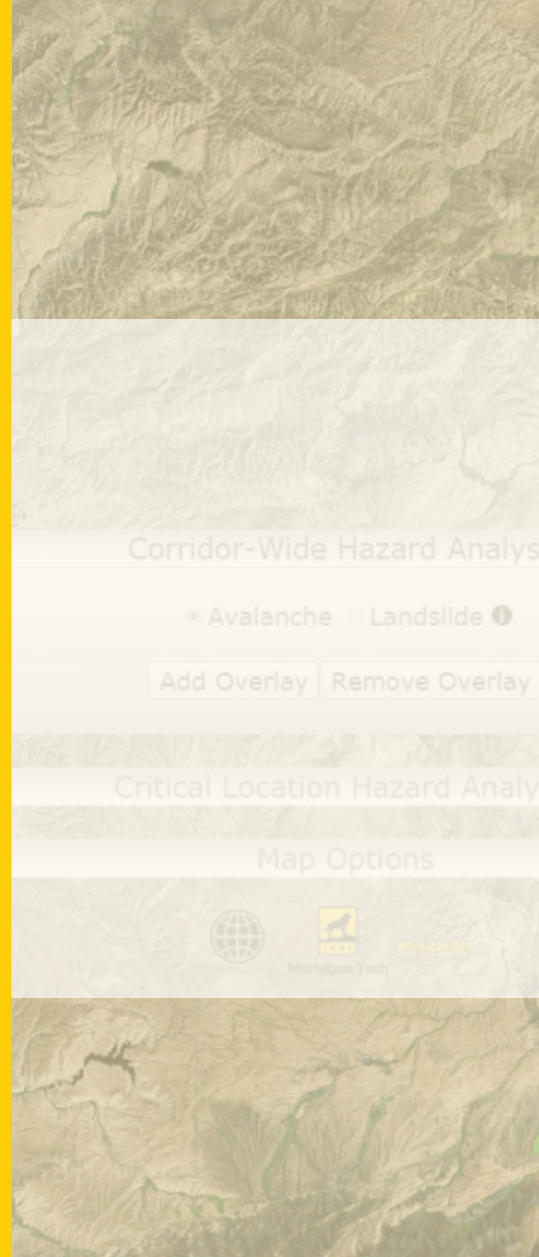
7. References

- Association of State Dam Safety Officials, "State Seismic Criteria. From ASDSO Survey on State-of-Practice References and Issues, November 1999. Association of State Dam Safety Officials" 2017. Visited online (June 2017): <http://www.damsafety.org/media/Documents/Surveys/1999SeismicCriteria.pdf>
- Baum, Rex L., William Z. Savage, and Jonathan W. Godt. "TRIGRS—a Fortran program for transient rainfall infiltration and grid-based regional slope-stability analysis." US geological survey open-file report 424 (2002): 38.
- Chowdhury, Robin, Phil Flentje, and Gautam Bhattacharya. Geotechnical slope analysis. Vol. 737. Balkema: Crc Press, 2010.
- Colorado Department of Transportation. 2017. "Avalanche Control". <https://www.codot.gov/travel/winter-driving/AvControl.html>. Accessed April 22, 2017.
- Fan, Ying, H. Li, and Gonzalo Miguez-Macho. "Global patterns of groundwater table depth." *Science* 339.6122 (2013): 940-943.
- Finlay, P. J., G. R. Mostyn, and R. Fell. "Landslide risk assessment: prediction of travel distance." *Canadian Geotechnical Journal* 36.3 (1999): 556-562.
- Hungr, Oldrich, Serge Leroueil, and Luciano Picarelli. "The Varnes classification of landslide types, an update." *Landslides* 11.2 (2014): 167-194.
- Hunter, Gavan, and Robin Fell. "Travel distance angle for rapid" landslides in constructed and natural soil slopes." *Canadian Geotechnical Journal* 40.6 (2003): 1123-1141.
- Jibson, Randall W. "Regression models for estimating coseismic landslide displacement." *Engineering Geology* 91.2 (2007): 209-218.
- Nobre, A. D., et al. "Height Above the Nearest Drainage—a hydrologically relevant new terrain model." *Journal of Hydrology* 404.1 (2011): 13-29.
- McClung, David M., and Peter A. Schaerer. 1980. "Snow avalanche size classification." *Proceedings of Avalanche Workshop*. Vol. 3. No. 5.
- Pelletier, Jon D., et al. "A gridded global data set of soil, intact regolith, and sedimentary deposit thicknesses for regional and global land surface modeling." *Journal of Advances in Modeling Earth Systems* (2016).
- Reid, Mark E., et al. "Scoops3D—Software to Analyze Three-Dimensional Slope Stability Throughout a Digital Landscape." *Tech. Rep. US Geological Survey Techniques and Methods*, book 14. 2015. 218.
- USGS, 2017. Shuttle Radar Topography Mission (SRTM) 1 Arc-Second Global. <https://lta.cr.usgs.gov/SRTM1Arc> (accessed, May 2017).

JUNE 29, 2017

Afghanistan Transportation Geohazard Mitigation and Investment Decision Support System

[HTTP://SPATIAL.MTRI.ORG/WBDSS](http://spatial.mtri.org/wbdss)



Michigan Tech

